Structural and Thermochemical Characterization of Lipoxygenase−Catechol Complexes†

Chau Pham,‡ Jerzy Jankun,§ Ewa Skrzypczak-Jankun,‡ Robert A. Flowers, II,‡ and Max O. Funk, Jr.*,‡

Departments of Chemistry and Medicinal and Biological Chemistry, University of Toledo, 2801 West Bancroft Street, Toledo, Ohio 43606, and Department of Urology and Physiology and Molecular Medicine, Medical College of Ohio, 3000 Arlington Avenue, P.O. Box 10008, Toledo, Ohio 43699

Received August 18, 1998; Revised Manuscript Received October 16, 1998

ABSTRACT: A complex between native, iron(II) soybean lipoxygenase 3 and 4-nitrocatechol, a known inhibitor of the enzyme, has been detected by isothermal titration calorimetry and characterized by X-ray crystallography. The compound moors in the central cavity of the protein close to the essential iron atom, but not in a bonding arrangement with it. The iron ligands experience a significant rearrangement upon formation of the complex relative to their positions in the native enzyme; a water molecule becomes bound to iron in the complex, and one histidine ligand moves away from the iron to become involved in a hydrogen bonding interaction with the catechol. These changes in position result in a trigonal pyramid coordination geometry for iron in the complex. Molecular modeling and force field calculations predict more than one stable complex between 4-nitrocatechol and the central cavity of lipoxygenase 3, but the interaction having the small molecule in the same orientation as the one found in the crystal structure was the most favorable. These observations reveal specific details of the interaction between lipoxygenase and a small molecule and raise the possibility that changes in the ligand environment of the iron atom could be a feature of the product activation reaction or the catalytic mechanism.

Lipoxygenase catalysis is an important aspect of polyunsaturated fatty acid metabolism in both plants and animals as the enzyme inaugurates the biosynthesis of several families of important mediators of physiological processes (*1*, *2*). The lipoxygenases from soybeans can be isolated in large amounts for detailed physical studies and have been extensively characterized (*3*). The soybean enzyme is a large (95 kDa) monomeric protein bearing a single non-heme iron cofactor. Spectroscopic studies (UV−vis, EPR,[1] Mössbauer, MCD, and EXAFS) have demonstrated that the iron atom plays a pivotal role in the catalytic mechanism (*4*−*8*). The lipoxygenases isolated from soybeans, referred to as native enzymes, contain iron(II). A reaction with the product of catalysis, 13(*S*)-hydroperoxy-9(*Z*),11(*E*)-octadecadienoic acid, results in conversion to iron(III) and concomitant activation of the enzyme. The product abolishes the distinctive lag phase observed in initial rate kinetic studies conducted with the native enzyme (*9*, *10*).

The rate-limiting step in lipoxygenase catalysis is hydrogen abstraction (*11*). Evidence for hydrogen tunneling in this step has been discovered in the form of very large, temperature-independent kinetic isotope effects (*12*). The catalytic cycle is completed when the intermediate formed in the rate-limiting step combines with molecular oxygen, and the product dissociates, leaving the enzyme in the iron(III) state for subsequent reaction cycles. While spectroscopic, kinetic, and even model studies have provided a wealth of information about the catalyzed reaction and the role that iron plays in it, the means by which the catalytic effect is achieved by the protein is still a matter for investigation.

The molecular basis for understanding lipoxygenase catalysis is just beginning to emerge. The structures of two soybean lipoxygenase isoenzymes and the rabbit reticulocyte enzyme have been determined recently by X-ray crystallography (*13*−*16*). The structures of these native proteins were found to consist of two domains, a smaller N-terminal eight-stranded β-barrel motif and a larger C-terminal, predominately α-helical domain. The iron atom is in a buried location within the larger domain, accessible from the surface of the molecule through hydrophobic channels or cavities. Molecular modeling of substrate binding has shown that a polyunsaturated fatty acid molecule can be accommodated in the channels near the iron site in a variety of ways.

The binding of small molecules to lipoxygenases, e.g., inhibitors, is of considerable practical importance because of the potential therapeutic value of lipoxygenase inhibition (*17*). The structure of the rabbit reticulocyte enzyme was obtained as a complex with the inhibitor RS75091 (*16*). The compound was located in one of the hydrophobic channels near the iron site. The carboxylate substituent of the inhibitor was found close to but not in a bonding interaction with the iron atom. The oxidation state of the rabbit enzyme in the

† This research was supported financially by a grant from the National Institutes of Health (GM 46522) and the DeArce Memorial Endowment for Biomedical Research at the University of Toledo.

‡ University of Toledo.

§ Medical College of Ohio.

[1] Abbreviations: EPR, electron paramagnetic resonance; MCD, magnetic circular dichroism; EXAFS, extended X-ray absorption fine structure; esff, extensible systematic force field.

10.1021/bi981989t CCC: $15.00
Published on Web 12/04/1998

crystals was presumably iron(II), the same as it was in the previously determined structures of the soybean lipoxygenases. These observations provided the first indications of how the native enzyme can interact with potential ligands.

Certain catechols are inhibitors of lipoxygenase catalysis (*18*). They form complexes with the iron(III) state of the enzyme. The 4-nitrocatechol complex, for example, has been characterized in spectroscopic and kinetic studies (*19*, *20*). The data were consistent with the stepwise formation of a bidentate iron−catecholate complex. The results of our investigation of the lipoxygenase−catechol interaction by X-ray crystallography, molecular modeling, and isothermal titration calorimetry are reported here. We find that the native, iron(II) lipoxygenase 3 interacts with catechols in a process that yields an apparent stoichiometry for binding of <1 in isothermal titration calorimetry experiments. A binding site was, however, identified in electron density difference maps from X-ray crystallographic data obtained from crystals of the native enzyme treated with catechol. The observed mode of catechol binding is supported by molecular modeling calculations. The position of the catechol in the lipoxygenase 3 complex, adjacent to the non-heme iron but at a nonbonding distance, is a reasonable candidate for the product binding site in the activation reaction.

MATERIALS AND METHODS

Materials. Lipoxygenase 3 was obtained from soybeans cv. Resnik by extraction, differential ammonium sulfate precipitation, dialysis, and chromatofocusing (*21*). The specific activity of the enzyme was at least 16 000 units mg^{-1} using linoleic acid solubilized with Tween 20 at pH 7.0 (*22*). 4-Nitrocatechol was obtained from Aldrich. 3,4-Dihydroxybenzonitrile was obtained from Lancaster. All other reagents were of the highest purity available.

Isothermal Titration Calorimetry. The enthalpy of binding was determined by titrating a 1.4 mL, 141 ± 8 μM solution of the enzyme with 3.8 ± 1 mM catechol in 0.1 M Tris-HCl buffer at pH 8.0 using an Omega titration calorimeter (MicroCal, Northampton, MA). The cell was thermostated to ±0.1 °C using a circulating bath. In all cases, the concentration of lipoxygenase 3 was determined using an ϵ_{280nm} of 120 000 L mol^{-1} cm^{-1} in 0.1 M Tris-HCl buffer at pH 8.0 and a monomer molecular mass of 95 000 Da (*22*). The enzyme was oxidized by treatment with the product of catalysis, 13-hydroperoxy-9(*Z*),11(*E*)-octadecadienoic acid, as previously described (*22*). Catechol solutions were prepared by weighing out a known amount of compound and dissolving it in 0.1 M Tris-HCl buffer at pH 8.0. The enthalpy of binding between catechol and lipoxygenase was determined from heats of multiple single injections. Injection volumes were 5 μL, and an equilibration time of 3 min was allowed between injections. The heat of dilution of each catechol in buffer was determined. The protein−catechol titration heat was adjusted by this small contribution.

The binding constant, *K*, and the number of binding sites, *n*, were obtained from the calorimetric data employing the Origin data analysis supplied with the Omega titration calorimeter. A complete description of the data analysis has been published (*23*).

Crystallography. Native lipoxygenase 3 crystals were soaked in a solution containing a 10-fold molar excess of 4-nitrocatechol for 20−40 h. The crystals turned a golden yellow color, and two were used for data collection. The measurements of the X-ray data for the structural analysis were taken on crystals mounted in Φ 1 mm glass capillaries on an RAXIS IV detector with dual plates and focusing mirrors, and a rotating Cu anode, set at 100 mA and 50 kV, using 2° oscillation frames with exposure of 15 min per frame and a 120 mm crystal-to-plate distance. Data were collected at room temperature to avoid a space group transition that accompanies freezing (*24*). A total of 183 617 reflections were processed and integrated together, giving 50 343 reflections to 2.15 Å resolution with 99% completeness and an R_{merge} (on *I*) of 7%. The structure was solved using the molecular replacement method with native lipoxygenase 3 as the starting model (PDB entry 1LNH with subtracted water molecules). The diffraction data were processed with Denzo and Scalepack (*25*). The refinement was conducted in X-plor (*26*).

Simulations. Molecular simulations were carried out on a Silicon Graphics Inc. Indigo2Impact computer using the InsightII program package from Molecular Simulations, Inc. (*27*). The protein, due to its size, had to be restricted to a sphere with a 20 Å radius around the iron atom. This volume contained the central cavity, and channels and allowed for movement of the catechol in this vicinity. The esff force field was used to assign the potentials and charges, and the modules Docking (in Discover) and Analysis were used to conduct the calculations and to evaluate the results. Hydrogen atoms were assigned according to pH 5.3, the pH at which the crystals were obtained and stored.

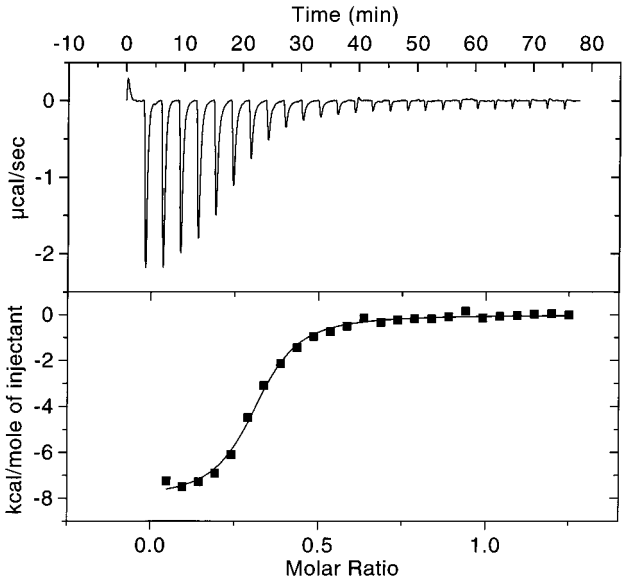

FIGURE 1: Isothermal titration calorimetry of native, iron(II) lipoxygenase 3 with 4-nitrocatechol. (Top) Heat change associated with addition of 5 μL aliquots of 4-nitrocatechol (3.8 mM) to lipoxygenase 3 (1.4 mL, 141 μM) and 0.1 M Tris-HCl at pH 8.0 and 27.0 °C. (Bottom) Binding isotherm.

RESULTS

Isothermal Titration Calorimetry of Lipoxygenase 3 with Catechols. Addition of aliquots of a 4-nitrocatechol solution to a solution of native lipoxygenase 3 at pH 8 in the microcalorimeter produced the binding isotherm shown in Figure 1. The thermodynamic parameters *n*, *K*, ΔH, ΔG, and

Table 1: Interaction between Iron(II) Lipoxygenase 3 and Catechols

parameter	4-nitrocatechol	3,4-dihydroxybenzonitrile
n	0.4 ± 0.1	0.17 ± 0.05
$K \times 10^{-5}$ (M^{-1})	5 ± 2	0.8 ± 0.3
ΔH (kcal mol^{-1})	-6 ± 1	-10 ± 2
ΔG (kcal mol^{-1})	-7.8 ± 0.2	-6.7 ± 0.2
ΔS (cal mol^{-1} K^{-1})	5 ± 4	-12 ± 7

Table 2: Interaction between Iron(III) Lipoxygenase 3 and Catechols

parameter	4-nitrocatechol	3,4-dihydroxybenzonitrile
n	1.29 ± 0.07	1.5 ± 0.1
$K \times 10^{-5}$ (M^{-1})	3 ± 2	2 ± 1
ΔH (kcal mol^{-1})	-9.1 ± 0.7	-10 ± 2
ΔG (kcal mol^{-1})	-7.5 ± 0.3	-7.2 ± 0.3
ΔS (cal mol^{-1} K^{-1})	-5 ± 3	-8 ± 8

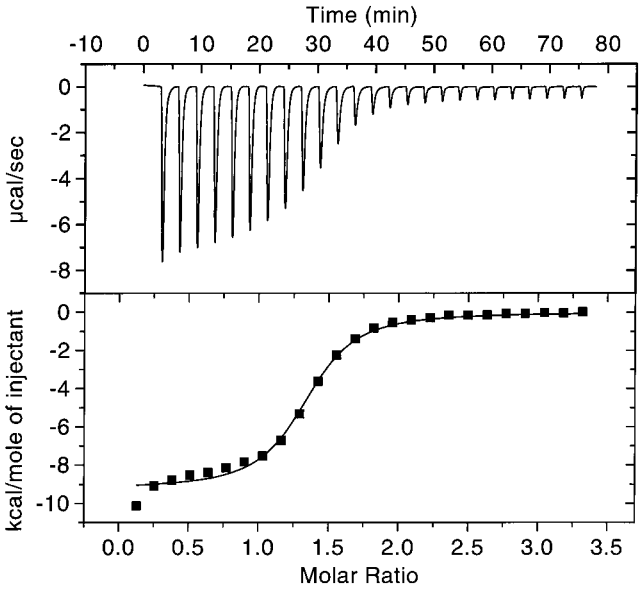

FIGURE 2: Isothermal titration calorimetry of iron(III) lipoxygenase 3 with 4-nitrocatechol. (Top) Heat change associated with addition of 5 μL aliquots of 4-nitrocatechol (3.8 mM) to product-oxidized lipoxygenase 3 (1.4 mL, 141 μM) and 0.1 M Tris-HCl at pH 8.0 and 27.0 °C. (Bottom) Binding isotherm.

ΔS extracted from the calorimetric data are contained in Table 1. Surprisingly, the calorimetric data showed that a substoichiometric amount of 4-nitrocatechol interacted with native lipoxygenase 3. The experiments were repeated numerous times and always resulted in substoichiometric ligand binding (25−50%). The interaction of 3,4-dihydroxybenzonitrile with native lipoxygenase 3 was also investigated and found to exhibit the same behavior. The results of these experiments are also described in Table 1. It is apparent from these data that the interaction of the ligand with lipoxygenase 3 is enthalpically driven in both cases and that 4-nitrocatechol has a higher affinity for native lipoxygenase 3 than 3,4-dihydroxybenzonitrile.

Oxidation of the iron atom in lipoxygenase 3 resulted in uptake of additional catechol. The thermodynamic parameters for 4-nitrocatechol and 3,4-dihydroxybenzonitrile are contained in Table 2, and the result of a typical titration experiment with 4-nitrocatechol is presented in Figure 2. The interaction of the ligands with oxidized lipoxygenase 3 is exothermic in both cases by approximately 9−10 kcal mol^{-1}, and the binding affinity (K) of both ligands is on the order of 1×10^5 M^{-1}. Although the ΔS is negative in both cases, the large error associated with this term makes analysis of the entropic component difficult. Regardless of this difficulty, it is clear that the association between the catechols and oxidized lipoxygenase 3 is enthalpically driven.

Crystallography of the Lipoxygenase−4-Nitrocatechol Complex. A summary of the experimental data is given in Table 3. The first electron density map, $F_o - F_c$, clearly showed the position and shape of the catechol moiety (Figure 3) and a possible shift in the position of the water molecule near the iron atom. Force field calculations were performed to guide the relative orientation of the catechol. The refinement indicates that catechol provides only partial occupancy and is not an iron ligand. Figure 4 illustrates the iron binding site [refinement in X-plor based on 41 149 reflections from 10 to 2.2 Å, $F_o > 2\sigma(F_o)$, 6709 non-hydrogen atoms, $R = 0.25$, $R_{free} = 0.31$ at this stage, and occupancy of 0.53 for 4-nitrocatechol[2]].

Assimilation of the catechol into the central cavity of the three-dimensional structure caused the relocation of the water molecule and the rearrangement of the amino acids at the iron binding site. The biggest change is for His-518. The imidazole ring is twisted away from the iron cofactor to participate in hydrogen bonds uniting the nitro group of the catechol with nearby residues: Asn-713 and the water molecule that binds to iron. The metal cofactor is coordinated by His-523, His-709, water, and the oxygen (OXT) from the C terminus of Ile-857. The other oxygen (O) from Ile-857 forms a hydrogen bond with one OH group from the catechol. The X-ray data therefore show that in the case of iron(II) the catechol does not bind to iron and does not have full occupancy, and its incorporation into the enzyme changes the neighborhood of iron and its coordination.

Molecular Simulations of the Lipoxygenase 3−4-Nitrocatechol Complex. To further assess the ligand−protein interaction, docking and energy minimization calculations were conducted for the assembly of lipoxygenase 3 and 4-nitrocatechol. After a series of fix docking calculations, three structures with the lowest potential energy were the subject of molecular dynamics calculations. The structures with the lowest potential energy were chosen as the most probable representatives for analysis of a variety of combinations of protonation and tautomeric states for the catechol. In all of the calculated structures, 4-nitrocatechol was positioned in the central cavity near the iron cofactor coincident with the unoccupied electron density in the difference map. The nitro group in 4-nitrocatechol was oriented away from the iron atom, and the hydroxyl groups, whether protonated or deprotonated, were turned toward the iron. The lowest potential energy as well as the lowest total energy was observed for dideprotonated 4-nitrocatechol. However, double dissociation at pH 5.3 for catechol not coordinated to iron seems unlikely to occur. The second lowest potential energy was observed for the structure deprotonated at the para position. The molecular dynamics calculations showed that structures resulting from deprotonation at the meta and para positions exhibited comparable total energies. The nonbonded intermolecular interactions between protein and 4-nitrocatechol were, however, stronger for the meta isomer. Therefore, it is possible that this form

[2] PDB code 1BYT.

Table 3: Statistical Evaluation of Data for Soybean Lipoxygenase 3 Crystals with 4-Nitrocatechol[a]

monoclinic, $C2$, $Z = 4$	native	with 4-nitrocatechol
a	112.8	112.9
b	137.4	137.5
c	61.9	61.9
β	95.5	95.5

shell limit (Å)			average		normal	linear R		completeness
upper	lower	I	error	stat	χ^2	factor	R^2	(%)
40.00	4.63	9344.9	259.5	101.0	2.300	0.044	0.052	92.5
4.63	3.68	8951.1	307.3	123.9	2.338	0.059	0.069	97.6
3.68	3.21	4589.8	237.7	116.5	1.545	0.073	0.079	99.4
3.21	2.92	2277.8	189.9	109.4	1.047	0.095	0.096	99.9
2.92	2.71	1353.7	172.2	107.0	0.783	0.124	0.120	100.0
2.71	2.55	944.7	153.6	105.2	0.725	0.153	0.148	99.9
2.55	2.42	709.0	151.0	105.3	0.635	0.184	0.171	99.8
2.42	2.32	536.7	149.8	107.0	0.595	0.229	0.211	99.7
2.32	2.23	421.1	158.8	109.1	0.516	0.278	0.255	99.7
2.23	2.15	326.6	152.7	109.7	0.514	0.346	0.310	99.3
all 50 343 reflections		2901.7	192.7	109.4	1.111	0.079	0.068	98.8

[a] Summary of intensities and R factors by shells. $R_{linear} = \Sigma|(I - \langle I\rangle)/\Sigma(I)$. $R^2 = \Sigma[(I - \times e1I\rangle)^2]/\Sigma(I^2)$. $\chi^2 = \Sigma[(I - \times e1I\rangle)^2]/[error^2 \times N/(N-1)]$.

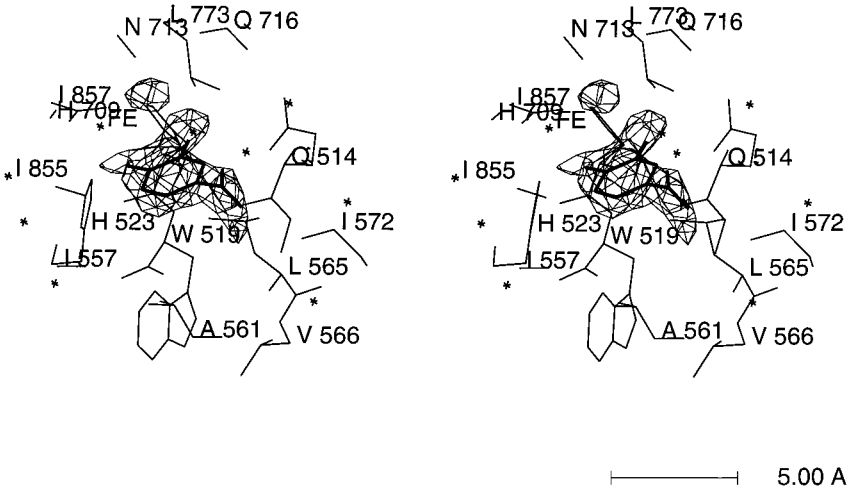

FIGURE 3: Electron density map ($F_o - F_c$) calculated with the protein model only showing the location of 4-nitrocatechol (stereoview).

is stabilized by lipoxygenase and represents the most probable structure.

DISCUSSION

Using isothermal titration calorimetry, an interaction between native, iron(II)-containing lipoxygenase 3 and two catechols has been detected. This technique is uniquely suited for this since the complex would not be expected to have any distinctive spectroscopic features. The substoichiometric ratio of ligand to protein obtained in the titrations was unanticipated. The reproducibility of the experiment provides convincing evidence that the values are correct. Further, oxidation of the enzyme to the active iron(III) form yields additional stoichiometric binding of the ligand as expected for the formation of a 1:1 complex (vide infra). The formation of a complex between catechol and native lipoxygenase is supported by the discovery of unassigned electron density which can be attributed to 4-nitrocatechol in electron density difference maps for crystals of the protein soaked with a solution of the catechol. Interestingly, the refinement points toward partial occupancy for the ligand in the protein molecules of the crystal. Molecular modeling further confirms the potential for the formation of a stable ligand protein complex, and the orientation of the catechol in each of the low-energy structures coincided with the crystal structure. It is therefore evident that at least a fraction of the lipoxygenase 3 molecules in the solid and solution samples formed complexes with catechols.

The less than stoichiometric association could be the result of an interaction that is more than a simple one-step association equilibrium. Nelson has previously demonstrated that iron(III) lipoxygenase 1 forms a 1:1 complex with catechols in a process that consists of at least two steps and may involve a noncovalent complex as one of the intermediates (*20*). Catechol binding to native lipoxygenase 3 at least in the crystals does not involve any significant conformational change in tertiary or secondary structure of the protein. Additional conformational states could represent discrete intermediates in the overall process. Aside from the presence of the density which can be attributed to the 4-nitrocatechol molecule and the rearrangement of residues in the iron binding site, the electron density difference maps do not reflect any significant differences in structure when the bound and free forms are compared. It is also possible that the stoichiometry reflects a lack of stability of the complex. For example, the formation of the catechol−iron(III) complex of lipoxygenase 1 gradually results in reduction of the cofactor and release of the semiquinone. It is hard to imagine

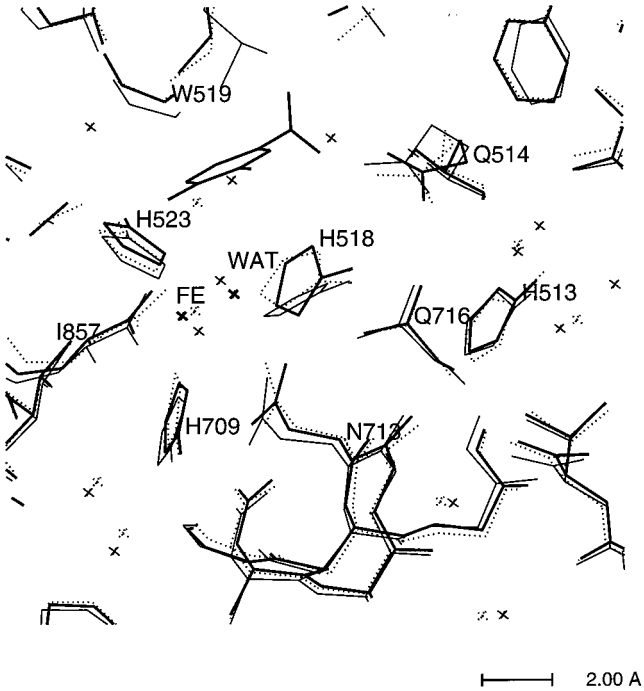

FIGURE 4: Comparison of the superimposed structures (Cα rmsd of <1 Å) of lipoxygenase 1 (thin line), native lipoxygenase 3 (dotted line), and the lipoxygenase 3−4-nitrocatechol complex (thick line).

what the corresponding chemistry would be for the iron(II) form of the enzyme, although molecular oxygen is not excluded from the titration experiments and could play a role. There is certainly no evidence for the formation of quinone in the UV−visible spectra of samples of the native enzyme treated with catechol in our experiments or in previous reports on this subject (*18*, *19*). The isothermal titration calorimetry experiments are by nature equilibrium measurements. Therefore, they cannot be expected to provide a description of the pathway for what may be a multistep process. They do however reveal for the first time a significant interaction between the catechols and native lipoxygenase 3. It was the observation of binding in the titrations that prompted us to consider crystal soaking experiments for the native enzyme with 4-nitrocatechol.

The conversion of iron(II) to iron(III) in lipoxygenase is accomplished by treatment of the enzyme with the product of catalysis, 13-hydroperoxy-9(*Z*),11(*E*)-octadecadienoic acid. The catechol complexes of iron(III) lipoxygenase 1 have been characterized in spectroscopic and kinetic studies (*18*, *20*). For example, the complexes have distinctive UV−visible, Raman, and X-ray absorption features. Further, the rate of the formation of the complexes revealed that the process occurs in steps with at least one intermediate. The spectroscopic evidence was consistent with the formation of a bidentate complex between the catechols and iron(III). The intermediate might involve either a monodentate iron−catechol interaction or a noncovalent complex. The isothermal titration experiments show that oxidized lipoxygenase 3 additionally binds approximately 1 mol more of each catechol in comparison to the native enzyme. This would be consistent with the formation of a 1:1 complex of the catechol with the iron atom. The protein apparently retains the ability to associate with catechol in a nonchelate fashion as the overall stoichiometry is >1 for the oxidized enzyme. In the lipoxygenase 3 isoenzyme structure, we previously found three channels (relative to two in the case of lipoxygenase 1) connecting the surface of the molecule with the iron site (*15*). Therefore, there are additional candidate sites for ligand binding in the lipoxygenase 3 molecule. Unfortunately, we do not yet have detailed structural information for the complexes of the oxidized form of the enzyme. Examination of the available space indicates that a second catechol molecule could approach the iron between His-709 and Asn-713. However, this requires some adjustments to avoid steric constraints in this area, and the calculated energy for such a complex is approximately 20 kcal/mol higher than that for the complex corresponding to the observed X-ray structure.

The crystallographic experiments on the lipoxygenase 3 complex with 4-nitrocatechol provide several new insights into the coordination environment of the critical iron cofactor. For example, an important issue in lipoxygenase chemistry is whether a water molecule is a ligand to iron. The current working hypothesis for the mechanism of action of lipoxygenases invokes proton abstraction from C11 (in linoleic acid) concomitant with electron transfer to the iron atom. Hydroxide bound to iron has been proposed to be the basic component of the enzyme (*28*). There is spectroscopic evidence for a water molecule bound to the iron(III) form of lipoxygenase 1 (*29*), and a bound water molecule was found in the crystal structure of lipoxygenase 1 determined at 100 K. The X-ray structures of lipoxygenase 1 and lipoxygenase 3 obtained at room temperature showed a solvent molecule approximately 4 Å from the metal cofactor, and no other molecules in the central cavity around the iron site, indicating highly dynamic disorder of solvent. In the lipoxygenase 3−4-nitrocatechol complex, a water molecule is within bonding distance of the iron atom and coincides with the position of the water molecule reported for lipoxygenase 1 at 100 K. A comparison of frozen lipoxygenase 1, native lipoxygenase 3, and its catechol complex (Figure 4) shows that catechol takes the place occupied by the solvent at 4 Å, pushing the water molecule toward iron to become a ligand.

The crystal structure also demonstrates that 4-nitrocatechol could be complexed to the enzyme without becoming coordinated to the iron atom. There are very few iron(II)−catechol complexes reported in the literature in comparison to iron(III) complexes which are numerous, and there are literally no thermodynamic data available for the associated equilibria (*30*, *31*). Therefore, there is little precedence for a strong bonding interaction, and one is not observed for the iron in native lipoxygenase 3 and 4-nitrocatechol.

The difference between the position of His-518 in the three-dimensional structure of the complex with 4-nitrocatechol and its location in the native protein is also notable as it represents a distinct change in the coordination sphere of the essential cofactor iron atom. His-518 is relocated from its previous position as an iron ligand. By twisting the imidazole ring away from iron, it forms a link in a tightly woven hydrogen bonding network (Figure 5) that incorporates the catechol and surrounds the iron site: Ile-857-OT1···*p*-OH-catechol-NO_2···ND1-His-518-NE2···OD2-N713-ND2···O-Leu-773/stacking interaction Phe-714···His-776/Glu-780-OE1···OG-Ser-856-Ile857-OT2-Fe and Asn-558-OD1···ND1-His-523-NE2-Fe-NE2-His-709. In this regard, it is also notable that in the native enzymes, both lipoxyge-

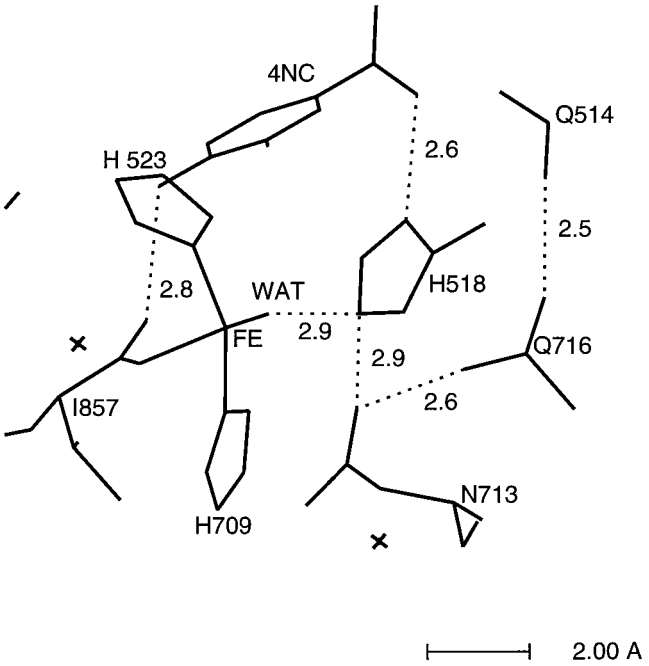

FIGURE 5: Hydrogen bonds near the iron binding site upon assimilation of 4-nitrocatechol.

nase 1 and lipoxygenase 3, His-518 has the highest temperature factor, i.e., the highest mobility, of all the iron ligands (*15*). His-518 is also oriented toward channel 2 and located near another conserved residue participating in local hydrogen bonding, His-513. While His-523, His-709, and Ile-857 anchor the iron from relatively fixed positions, His-518 and Asn-713 show considerable mobility in response to the circumstances. As a result, the geometry of the iron coordination sphere is changing as well. In the lipoxygenase 3−4-nitrocatechol complex, it resembles a distorted trigonal pyramid with His-523-NE2, His-709-NE2, and water at the base (average angle of 117°), Ile-857-OT2 in the axial position (average angle of 100°), and iron shifted approximately 0.5 Å toward Ile-857. This geometry has been observed before in superoxide dismutase and was shown to be vulnerable not to changes in the oxidation state of iron but to the incorporation of a small molecule (azide in that case) into the crystal structure (*32*).

In summary, we have shown that (1) water can coordinate to the iron(II) form of lipoxygenases under conditions promoting order, such as suppressing available space by incorporation of 4-nitrocatechol or by freezing, (2) the catechol can form a complex with the enzyme without forming a bond to the iron, and (3) changes in the conformation of side chains near the iron upon formation of a complex result in differences in coordination. These observations raise the prospect that ligand mobility could be an element of the catalytic mechanism or the activation process.

REFERENCES

1. Samuelsson, B., Dahlen, S.-E., Lindgren, J. A., Rouzer, C. A., and Serhan, C. N. (1987) *Science 237*, 1171−1176.
2. Creelman, R. A., and Mullet, J. E. (1997*) Annu. Rev. Plant Phys. Plant Mol. Biol. 48*, 355−381.
3. Solomon, E. I., Zhou, J., Neese, F., and Pavel, E. G. (1997) *Chem. Biol. 4*, 795−808.
4. De Groot, J. J. M. C., Garssen, G. J., Veldink, G. A., Vliegenthart, J. F. G., Boldingh, F., and Egmond, M. R. (1975) *FEBS Lett. 56*, 50−54.
5. De Groot, J. J. M. C., Veldink, G. A., Vliegenthart, J. F. G., Boldingh, J., Wever, R., and Van Gelder, B. F. (1975) *Biochim. Biophys. Acta 377*, 71−79.
6. Funk, M. O., Carroll, R. T., Thompson, J. F., Sands, R. H., and Dunham, W. R. (1990) *J. Am. Chem. Soc. 112*, 5375−5376.
7. Pavlosky, M. A., and Solomon, E. I. (1994) *J. Am. Chem. Soc. 116*, 11610−11611.
8. Scarrow, R. C., Trimitsis, M. G., Buck, C. P., Grove, G. N., Cowling, R. A., and Nelson, M. J. (1994) *Biochemistry 33*, 15023−15035.
9. Haining, J. L., and Axelrod, B. (1958) *J. Biol. Chem. 232*, 193−202.
10. Schilstra, M. J., Veldink, G. A., and Vliegenthart, J. F. G. (1994) *Biochemistry 33*, 3974−3979.
11. Hamberg, M., and Samuelsson, B. J. (1967) *J. Biol. Chem. 242*, 5329−5335.
12. Moiseyev, N., Rucker, J., and Glickman, M. H. (1997) *J. Am. Chem. Soc. 119*, 3853−3860.
13. Boyington, J. C., Gaffney, B. J., and Amzel, L. M. (1993) *Science 260*, 1482−1486.
14. Minor, W., Steczko, J., Stec, B., Otwinowski, Z., Bolin, J. T., Walter, R., and Axelrod, B. (1996) *Biochemistry 35*, 10687−10701.
15. Skrzypczak-Jankun, E., Amzel, L. M., Kroa, B., and Funk, M. O. (1997) *Proteins: Struct., Funct., Genet. 29*, 15−31.
16. Gillmor, S. A., Villasenor, A., Fletterick, R., Sigal, E., and Browner, M. F. (1997) *Nat. Struct. Biol. 4*, 1003−1009.
17. Bell, R. L., Summers, J. B., and Harris, R. R. (1997) *Annu. Rep. Med. Chem. 32*, 91−100.
18. Spaapen, L. J. M., Verhagen, J., Veldink, G. A., and Vliegenthart, J. F. G. (1980) *Biochim. Biophys. Acta 617*, 132−140.
19. Nelson, M. J. (1988) *Biochemistry 27*, 4273−4278.
20. Nelson, M. J., Brennan, B. A., Chase, D. B., Cowling, R. A., Grove, G. N., and Scarrow, R. C. (1995) *Biochemistry 34*, 15219−15229.
21. Funk, M. O., Carroll, R. T., Thompson, J. F., and Dunham, W. R. (1986) *Plant Physiol. 82*, 1139−1144.
22. Draheim, J. E., Carroll, R. T., McNemar, T. B., Dunham, W. R., Sands, R. H., and Funk, M. O. (1989) *Arch. Biochem. Biophys. 269*, 208−218.
23. Wiseman, T., Williston, S., Brandts, J. F., and Lin, L.-N. (1989) *Anal. Biochem. 179*, 131−137.
24. Skrzypczak-Jankun, E., Bianchet, M. A., Amzel, L. M., and Funk, M. O. (1996) *Acta Crystallogr. D52*, 959−965.
25. Otwinowski, Z., and Minor, W. (1997) *Methods Enzymol. 276*, 307−326.
26. Brunger, A. T. (1992) *X-plor Version 3.1. A System for X-ray Crystallography and NMR*, Yale University Press, New Haven, CT.
27. Molecular Simulations, Inc. (1995) *InsightII, Version 95.0/3.0.0, User's Guide*, San Diego, CA.
28. Nelson, M. J., and Seitz, S. P. (1994) *Curr. Opin. Struct. Biol. 4*, 878−884.
29. Nelson, M. J. (1988) *J. Am. Chem. Soc. 110*, 2985−2986.
30. Shoner, S. C., and Power, P. P. (1992) *Inorg. Chem. 31*, 1001−1010.
31. Chiou, Y.-M., and Que, L. (1995) *Inorg. Chem. 34*, 3577−3578.
32. Lah, M. S., Dixon, M. M., Pattridge, K. A., Stallings, W. C., Fee, J. A., and Ludwig, M. L. (1995) *Biochemistry 34*, 1646−1660.

BI981989T